Pore Induction in Human Epidermal Membrane during Low to Moderate Voltage Iontophoresis: A Study Using AC Iontophoresis

S. KEVIN LI,* ABDEL-HALIM GHANEM, KENDALL D. PECK, AND WILLIAM I. HIGUCHI

Contribution from *Department of Pharmaceutics and Pharmaceutical Chemistry, University of Utah, Salt Lake City, Utah 84112.*

Received August 13, 1998. Accepted for publication December 18, 1998.

Abstract □ The present study aimed to investigate new pore induction as a flux-enhancing mechanism in human epidermal membrane (HEM) with low to moderate voltage electric fields. The extent of pore induction and the effective pore sizes of these induced pores were to be assessed using a low frequency (12.5 Hz) low to moderate voltage (2.0 to 4.0 V) square-wave alternating current (ac) "passive" permeation method (ac iontophoresis). This ac approach was to allow for inducing and sustaining a state of pore induction in HEM while permitting no significant transport enhancement via electroosmosis; thus, transport enhancement entirely due to new pore induction (enhanced passive permeation) was to be assessed without any contributions from electroosmosis. Good proportionality between the increase in HEM permeability and its electrical conductance was found with the "passive" transport data obtained during square-wave ac iontophoresis using urea as the model permeant. Typically, at 3.0 to 4.0 V, HEM conductance increases (and permeability increases) ranged from around 3- to 30-fold. These results appear to be the first *direct* evidence that new pore induction in HEM is a significant flux enhancing mechanism under moderate voltage conditions. The extents of pore induction in HEM under low frequency moderate voltage (2.0 to 3.0 V) ac, pulsed direct current (dc), and continuous dc were also compared. The extents of pore induction from square-wave ac and pulsed dc were generally of the same order of magnitude but somewhat less than that observed during continuous dc iontophoresis at the same applied voltage and duration, suggesting less extent of pore induction with reversing polarity or when a brief delay is provided between pulses to allow for membrane depolarization. The average effective pore sizes calculated for the induced pores from the experimental data with urea and mannitol as probe permeants and the hindered transport theory were 12 ± 2 Å, which are of the same order of magnitude as those of preexisting pores determined from conventional passive diffusion experiments.

Introduction

Previous studies have provided insights regarding iontophoretic transdermal transport mechanisms of ionic and polar compounds with human epidermal membrane (HEM). It has been shown that the alteration of HEM barrier properties during low to moderate voltage iontophoresis is consistent with the induction of new pores (or new pathways) with the observed increase in HEM electrical conductance correlating with the increase in HEM permeability.[1] The occurrence of pore induction during low to moderate voltage iontophoresis was hypothesized in even earlier studies,[2−5] but other explanations for the decrease in electrical resistance and the increase in permeability during iontophoresis could not be justifiably excluded.[5−9] Also, some recent reports have continued to take the view that significant new pore induction in HEM can occur only at high voltages and that (at conventional voltages employed in iontophoresis) "iontophoresis primarily involves electrically driven transport through *fixed* pathways across the stratum corneum".[10−12]

In a recent study with HEM, the size of the pores induced during low to moderate voltage iontophoresis was estimated with neutral permeants in electroosmosis experiments.[13] However, because electroosmosis depends on the sign and magnitude of the pore surface charge density, pore size estimation based on these data are considered to be compromised by possible variable pore surface charge density in HEM.

As will be shown, square-wave ac iontophoresis can be used as a tool in characterizing the barrier properties of human skin during iontophoresis and pore induction. A method based on ac iontophoresis may be employed to study the state of pore induction in the absence of flux enhancement from electroosmosis and from electrophoresis. Particularly, the characteristics of the pores induced in HEM during iontophoresis (pulsed dc, square-wave ac, and/or continuous dc) may be investigated with this ac iontophoresis strategy regardless of possible pore surface charge distributions because transport enhancement due to pore induction can be isolated from the additional enhancement due to electroosmosis and electrophoresis.

The present study aimed to investigate pore induction as a flux-enhancing mechanism during low to moderate applied voltage iontophoresis with HEM. An ac "passive" permeation method (i.e., square-wave ac iontophoresis) was to be developed and used to quantify the extent of pore induction and the effective size of the pores induced. The effects of square-wave ac and pulsed dc on the barrier properties of HEM were also to be compared with continuous dc iontophoresis.

Experimental Section

Materials—Radiolabeled [^{14}C]urea and [^{3}H]mannitol were purchased from New England Nuclear (Boston, MA) and American Radiolabeled Chemicals (St. Louis, MO). Human epidermal membrane (HEM) was supplied by TheraTech Inc. (Salt Lake City, UT). HEM was prepared by heat separation[14] with human skin (from the back, abdomen, or thigh) obtained from Ohio Valley Tissue and Skin Bank (Cincinnati, OH) and was frozen immediately for later used. Millipore GVWP filters (0.22 μm pore diameter) were purchased from Millipore Corporation (Bedford, MA). Phosphate-buffered saline (PBS) at 0.1 M ionic strength and pH 7.4 containing 0.02% sodium azide was prepared by reagent grade chemicals and distilled deionized water.

General Experimental Setup—Iontophoresis studies were carried out in a side-by-side two-chamber diffusion cell (diffusional surface area of around 0.8 cm^2 and chamber volume of 2 or 4 mL) using a four-electrode potentiostat system (JAS Instrumental Systems, Inc., Salt Lake City, UT) as described previously[15] and a waveform programmer (JJ 1276, JAS Instrument Systems, Inc., Belmont, NC) at 37 °C. The counter electrodes were Ag−AgCl. Unless otherwise specified, dc iontophoresis was conducted with

* To whom correspondence should be addressed. E-mail address: kevin.li@m.cc.utah.edu.

10.1021/js980331y CCC: $18.00 Published on Web 02/20/1999

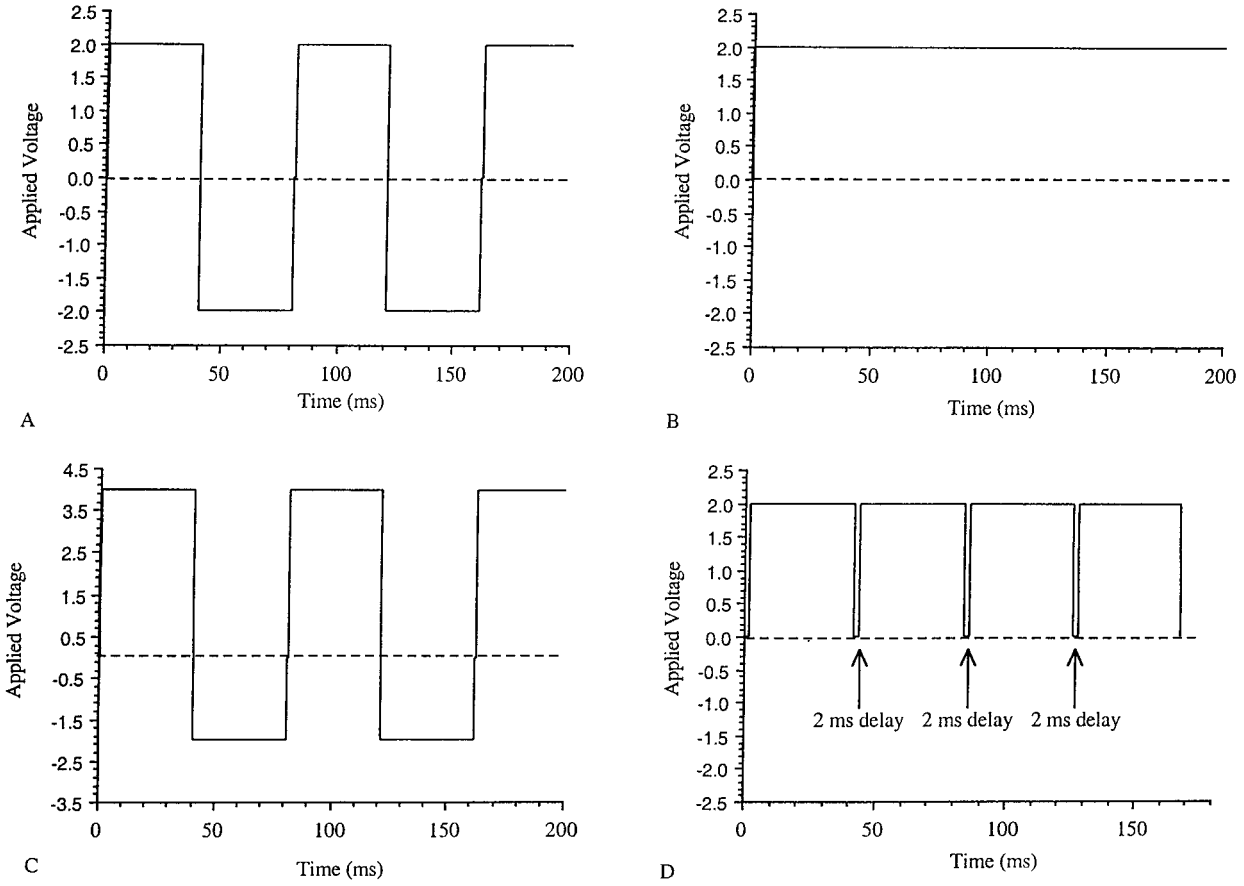

Figure 1—Representative waveform diagrams. (A) 2.0 V 12.5 Hz square-wave ac iontophoresis, (B) 2.0 V continuous dc iontophoresis, (C) superposition of a 1.0 V dc and 12.5 Hz 3.0 V square-wave ac iontophoresis, (D) 2.0 V pulsed dc iontophoresis with 2 ms delay.

the anode in the donor chamber and cathode in the receiver chamber. The electrical conductance of the membrane was monitored by an oscilloscope (Model 2211, Tektronix Inc., Beaverton, OR). Initial electrical conductance was determined by applying a 100 mV potential drop across the membrane. In each transport experiment, the receiver and donor chambers were filled with PBS and PBS premixed with tracer levels of radiolabeled permeants. An appropriate amount of receiver solution sample (1 mL sample for the 2 mL diffusion cells and 1 or 2 mL for the 4 mL diffusion cells) was withdrawn at predetermined time intervals and replaced with fresh PBS, and a 10 μL donor sample was also withdrawn at the same time. These samples were mixed with 10 mL of scintillation cocktail (Ultima Gold, Packard, Meriden, CT) and assayed in a liquid scintillation counter. The apparent permeability coefficients (P) in each experiment were calculated by:

$$P = \frac{1}{C_D A}\frac{dQ}{dt} \quad (1)$$

where A is the membrane surface area, t is time, Q is the amount of permeant transported into the receiver chamber, and C_D is the concentration of permeant in the donor chamber. The pH of the solutions in the donor and receiver chambers was checked after each iontophoresis run.

Nuclepore Membrane Studies—Nuclepore membranes (polycarbonate membrane, 7.5 nm pore radius, 0.001 porosity) were used (the control) to examine the "passive" permeation technique (i.e., square-wave ac iontophoresis) before applying the method to HEM. An assembly of 50 Nuclepore membranes (Nuclepore Corp., Pleasanton, CA) was mounted between the two side-by-side diffusion half-cells. These studies were divided into two stages with mannitol as the permeant. Stage I was passive permeation. In stage II, one of the following protocols was carried out: square-wave ac iontophoresis (amplitude of 1.0 or 2.0 V and frequency ranging from 1.25 to 50 Hz), continuous 0.5 V dc iontophoresis, or a protocol of superposition of 12.5 Hz 2.0 V ac and 0.5 V continuous dc iontophoresis. The duration of the ac transport experiments was around 3 to 5 h. Representative waveforms are shown in Figure 1. Radiolabeled [^{3}H]mannitol was the model permeant in the experiments.

HEM Electrical Resistance Studies—Prior to carrying out the HEM permeant transport studies, a set of experiments were conducted to assess the extent of pore induction in HEM under the low frequency (12.5 Hz) ac voltage regimens and to compare the results to continuous dc and pulsed dc regimens. See General Experimental Setup. HEM supported with a Millipore filter[16] was mounted between the two half-cells of the diffusion cell. HEM was allowed to equilibrate in PBS at 37 °C for 12 to 40 h until its conductance became essentially constant with time before the experiments. The purpose of incubating HEM in PBS was to establish a steady baseline (an essentially constant HEM conductance with time, determined with 100 mV) for comparison studies; changes in HEM electrical conductance are generally observed in the first 10 h (sometimes up to 20 h) of the incubation even though HEM conductance usually does not change by more than a factor of 2 (usually decreases and sometimes increases) during this period. It has been shown that after this equilibration phase, the barrier properties of HEM can remain stable for up to 5–7 days.[16] After this equilibration phase, the following protocol of consecutive runs with a given HEM was employed: 2.0 V 12.5 Hz square-wave ac (which is alternating 40 ms pulses) for 10 s; 2.0 V 40 ms square-wave dc pulses with 1, 2, or 3 ms delay between pulses for 10 s; continuous 2.0 V dc for 10 s; then returning back to 2.0 V 12.5 Hz ac for 10 s. Other similar protocols were also employed with the first and last runs always the same to ensure reversibility/reproducibility in a given set of consecutive runs with a single HEM. Similar experiments were carried out with 3.0 V instead of 2.0 V. HEM electrical resistance was monitored by measuring the current[17] with the oscilloscope throughout the sequence of runs.

HEM Transport Studies—For the iontophoresis/transport studies with HEM, the same experimental setup was used (as above). The receiver and donor chambers were filled with PBS and PBS premixed with trace amounts of the radiolabeled [^{3}H]mannitol

and/or [^{14}C]urea. Mannitol and urea were chosen as the model permeants in the present study because they have well-characterized diffusion properties and are polar nonelectrolytes that essentially transport across the stratum corneum via the pore pathways.[14,18] The apparent permeability coefficients for HEM were calculated with eq 1. The present HEM investigation was divided into three levels of analyses (studies A, B, and C). In study A, the effective radii of the pores induced during square-wave ac iontophoresis were deduced and compared with those of the preexisting pores. In study B, a 1 min 4.0 V prepulse was provided before the square-wave ac run to better match the extent of pore induction to that with continuous dc iontophoresis because the extent of pore induction under continuous dc iontophoresis was generally found to be somewhat higher than that under the same voltage ac iontophoresis (see HEM Electrical Resistance Studies in the Results section and Pulsed and Continuous Iontophoresis in the Discussion section). The objective of study C was to examine whether the pores induced under square-wave ac iontophoresis are similar to those induced under continuous dc iontophoresis.

As part of study A, some preliminary experiments were performed with urea as the only probe permeant. These experiments with urea alone were aimed to establish a HEM permeability vs resistance correlation for square-wave ac iontophoresis. The main experiments in study A were done using urea and mannitol as dual permeants to permit estimating the effective radii of the induced pores. Study A involved three stages. Stage I was a passive permeation run. Stage II was 2.0 V 12.5 Hz square-wave ac and 3.0 V 12.5 Hz square-wave ac iontophoresis when urea was involved alone and when urea and mannitol were the dual permeants, respectively. The duration of stage II ranged from 2 to 5 h depending on the electrical resistance of HEM (around 2 h for the lower resistance and around 5 h for the higher resistance HEM samples). Stage III was a passive permeation run carried out again after the iontophoresis run when the electrical resistance of HEM became constant with time.

Study B also involved three stages. Stage I was passive transport run. Stage II was 4.0 V dc iontophoresis for 1 min (prepulse) followed by a square-wave ac iontophoresis run (3.0 or 4.0 V at 12.5 Hz) for a duration ranging from 1.5 to 6 h. Again, stage III was a passive permeation experiment after iontophoresis when the electrical resistance of HEM became constant with time.

Study C involved five stages. Stage I was a passive permeation run. Stage II was continuous dc iontophoresis (2.0 or 3.0 V; duration of around 0.5 to 1.5 h). Immediately after the continuous dc iontophoresis, stage III was square-wave ac iontophoresis (3.0 or 4.0 V at 12.5 Hz; around 2 to 6 h) following a 4.0 V dc 1 min prepulse. In stage IV, square-wave ac iontophoresis (3.0 or 4.0 V at 12.5 Hz) was superimposed over 1.0 V continuous dc for a duration ranging from around 1.5 to 3 h. The various waveforms used in stages II, III, and IV are illustrated in Figure 1. Stage V was a passive permeation run after the electrical resistance of HEM became constant with time.

Theory and Effective Pore Radius Calculation—Methods of estimating the effective pore radii for the pore pathway in HEM have been described previously for passive permeation[18] and iontophoresis[13] using the hindered transport theory. Briefly, the steady-state iontophoretic flux ($J_{\Delta\psi}$) for a nonionic permeant through HEM can be described by a convective transport model derived from the modified Nernst–Planck theory:[13]

$$J_{\Delta\psi} = \frac{C_D \epsilon W v}{1 - \exp[-Wv(\Delta x)/(HD)]} \quad (2)$$

where ϵ is the combined porosity and tortuosity factor for the membrane, v is the average velocity of the convective solvent flow, H and W are the hindered transport factors for passive diffusion and for transport due to the convective solvent flow induced by electroosmosis, Δx is the effective membrane thickness, C_D has been previously defined in eq 1, and D is the permeant diffusion coefficient taken from the literature.[18] Assuming a single pore size (radius, R_p) and a cylindrical pore geometry in the membrane, the hindrance factor for Brownian diffusion (H) and the hindrance factor for pressure-induced parabolic convective solvent flow (W) can be expressed by:[19]

$$H(\lambda) = (1 - \lambda)^2(1 - 2.104\lambda + 2.09\lambda^3 - 0.948\lambda^5) \quad (3)$$

$$W(\lambda) = (1 - \lambda)^2(2 - (1 - \lambda)^2)\left(1 - \frac{2}{3}\lambda^2 - 0.163\lambda^3\right) \quad (4)$$

when the ratio of solute radius to pore radius (r/R_p) is small (i.e. $\lambda = r/R_p < 0.4$). The hydration radii (Stokes–Einstein radii, r) of the permeants can be obtained from the literature.[18]

At the convection limit (convective flow transport ≫ passive diffusion), eq 2 reduces to:

$$J_{\Delta\psi} = \epsilon W v C_D \quad (5)$$

In the case of passive diffusion, the appropriate relation is:

$$J_{\text{passive}} = \frac{DC_D\epsilon H}{\Delta x} \quad (6)$$

Fluxes for nonionic permeants with square-wave ac iontophoresis in the present study are expected to be well approximated by eq 6, because the electroosmosis contribution to the flux is expected to be negligible at the ac frequencies used (see Nuclepore Membrane Studies in the Results section and the last paragraph in HEM Transport Studies in the Discussion section). In this situation, the effective pore radii for HEM can be estimated from the ratio of urea and mannitol fluxes with eq 6 as in the passive diffusion experiments:

$$\frac{J_m}{J_u} = \frac{H_m}{H_u}\frac{D_m}{D_u} \quad (7)$$

where the subscripts m and u represent the probe permeants mannitol and urea, respectively. The limitations of eqs 5–7 and the uncertainties of estimating the effective pore radii have been previously discussed.[13,18]

The electrical resistance of HEM (R) in PBS is expected to be proportional to its thickness and inversely proportional to its effective porosity:

$$R \propto \frac{\Delta x}{\epsilon H} \quad (8)$$

From eqs 6 and 8 and taking logarithms,

$$\log P = -\log R + c \quad (9)$$

where c is a constant. Equation 9 shows that the electrical resistance of HEM can be expressed as a function of its permeability for the conducting ions. A plot of the logarithm of the permeant permeability coefficient of a membrane vs the logarithm of membrane electrical resistance yielding a slope of − 1.0 would therefore suggest similar transport pathways for the permeant and the conducting ions across the membrane under the specified experimental conditions.

Results

Nuclepore Membrane Studies—The studies with Nuclepore membrane (Figure 2) served to validate the instrumentation (i.e., the four electrode potentiostat system and the waveform programmer) and provided a baseline for the transport studies with HEM. The resistance of an assembly of 50 Nuclepore membranes was found to be essentially the same over the range of applied voltage conditions and the frequency range in the present study (data not shown). The plateau value of the current observed on the oscilloscope display after a brief (within 1 ms) transient period was used to calculate the electrical resistance (the resistance portion of a parallel capacitance and resistance model circuit[20]). Results for mannitol transport with square-wave ac iontophoresis (ranging from 1.25 to 50 Hz), continuous dc iontophoresis (0.5 V), and square-wave ac (2.0 V at 12.5 Hz) superimposed with continuous dc iontophoresis (0.5 V) are summarized in Figure 2. As can be seen, the mannitol

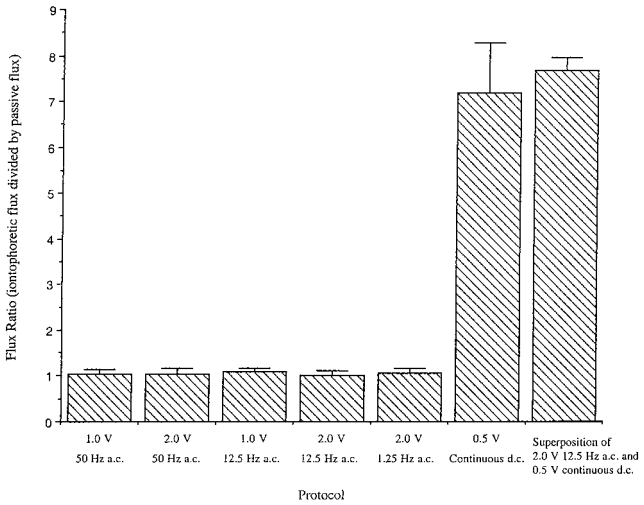

Figure 2—Mannitol flux ratios (iontophoretic flux divided by passive flux) during square-wave ac iontophoresis, continuous dc iontophoresis, and superposition of 12.5 Hz square-wave ac and continuous dc iontophoresis for an assembly of 50 Nuclepore membranes are plotted against the respective experimental protocols. Each bar represents the mean and standard deviation of $n \geq 3$.

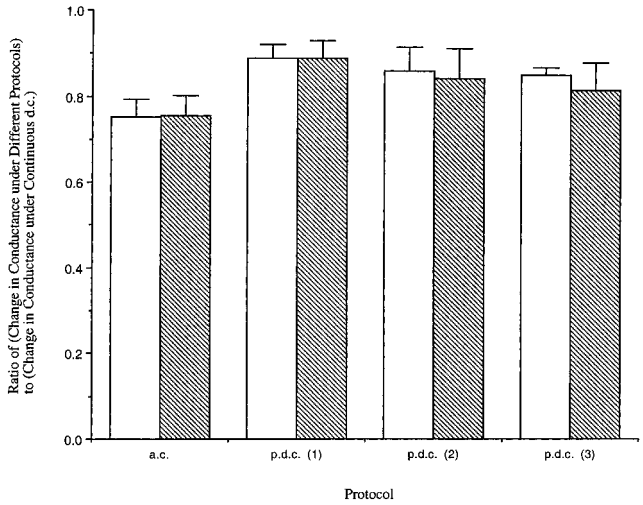

Figure 3—Effects of square-wave ac and pulsed dc iontophoresis on the barrier properties of HEM relative to those of continuous dc at 2.0 V (open bar) and 3.0 V (striped bar). The changes in HEM conductance under different protocols divided by the changes in conductance during continuous dc iontophoresis (for individual HEM samples) were plotted against different protocols. Changes in conductance were determined by conductance (i.e., $1/R$ ($1/k\Omega$)) at 10 s into the iontophoresis run minus the conductance before the iontophoresis run. Abbreviations: ac, 12.5 Hz square-wave ac iontophoresis; pdc, 40 ms square-wave pulsed dc iontophoresis with a brief delay (numbers, ms, in brackets) between each pulse. Each data bar represents the mean ± 95% confidence interval ($n \geq 3$).

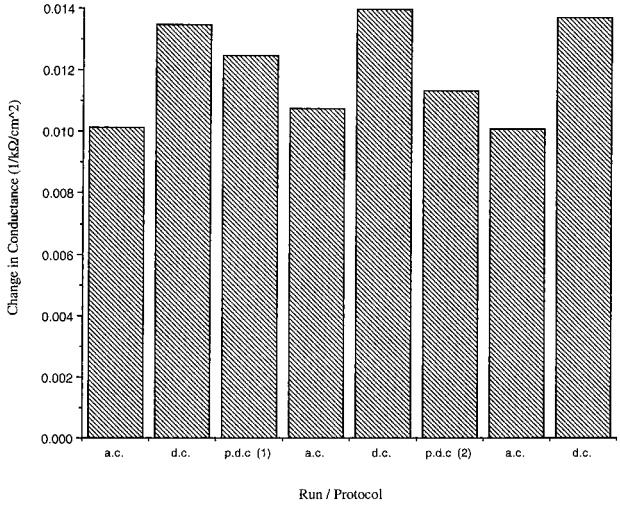

Figure 4—Representative data from a 2.0 V HEM resistance study with a single HEM. The initial electrical resistance of this HEM sample was 71 kΩ cm^2. The HEM electrical resistance just before an iontophoresis run (original or after recovery from the preceding run) was 72 ± 3 kΩ cm^2 (mean ± SD, ranging from 68 to 75 kΩ cm^2). The changes in HEM electrical conductance (changes in $1/R$ from before to the end of the iontophoresis run) are plotted against the different iontophoresis protocols from left to right in the order in which they were carried out. Abbreviations: ac, 12.5 Hz square-wave ac iontophoresis; dc, continuous dc iontophoresis; pdc, 40 ms square-wave pulsed dc iontophoresis with a brief delay (numbers, ms, in brackets) between each pulse.

fluxes with square-wave ac iontophoresis at the voltage conditions in the present study and at frequency ranging from 1.25 to 50 Hz were essentially the same as the fluxes in passive diffusion, in good agreement with predictions based on eq 6 as discussed earlier. This demonstrates that, at sufficiently high frequencies (≥1.25 Hz in the case of the present Nuclepore membrane) under the applied voltage conditions and duration studied, ac iontophoresis does not enhance the transport of permeants across membranes. The results in Figure 2 represent the concept underpinning the HEM studies in the next section.

The flux enhancement with 0.5 V continuous dc superimposed with square-wave ac (2.0 V at 12.5 Hz) was essentially the same as that with 0.5 V continuous dc iontophoresis. The fluxes with 0.5 V continuous dc iontophoresis were more than 7 times higher than those with square-wave ac iontophoresis and passive diffusion; the enhancement factor determined in the present 0.5 V continuous dc iontophoresis experiments is consistent with previous results.[21]

HEM Electrical Resistance Studies—Figure 3 summarizes the results of the experiments designed to compare the extent of pore induction in HEM during 12.5 Hz ac and pulsed dc iontophoresis with continuous dc iontophoresis. A total of 19 HEM samples were involved in this study, with each sample taken successively through several 10 s runs as described in the Experimental section. Figure 4 shows representative results of consecutive experimental runs with a HEM sample. As can be seen in Figure 3, the increases in the electrical conductance with 12.5 Hz ac and with pulsed dc were generally less than (Student's *t*-test of 95% confidence level), but of the same order of magnitude of that observed with continuous dc at the same applied voltages (2.0 or 3.0 V). In general, the increase in the electrical conductance with 12.5 Hz ac was around 75% of that with continuous dc. In these experiments, as the delay time between pulses was increased, the pore induction approached that found with 12.5 Hz ac.

HEM Transport Studies—Typical examples of transport enhancement results of studies A and C are presented in Figures 5 and 6, respectively. Figure 5 gives data of urea flux and electrical conductance for stage II of study A, where 3.0 V 12.5 Hz square-wave ac was applied for approximately 250 min. As can be seen here, both the electrical resistance and the corresponding flux generally attained near plateau values within 1 h, the plateaus representing around an 8-fold increase in conductance relative to the initial value. Results similar to those in study A were observed in study B. In the example presented in Figure 6 (an example of study C), stage II was 2.0 V dc iontophoresis for around 50 min; stage III was 4.0 V dc for 1 min followed by 3.0 V square-wave ac iontophoresis for 2 h; stage IV was superposition of 1.0 V dc over 3.0 V 12.5 Hz ac iontophoresis. It is seen in this example that there was significant pore induction during stage II but little or no further change in the state of pore induction during stages III and IV. Also can be noted in

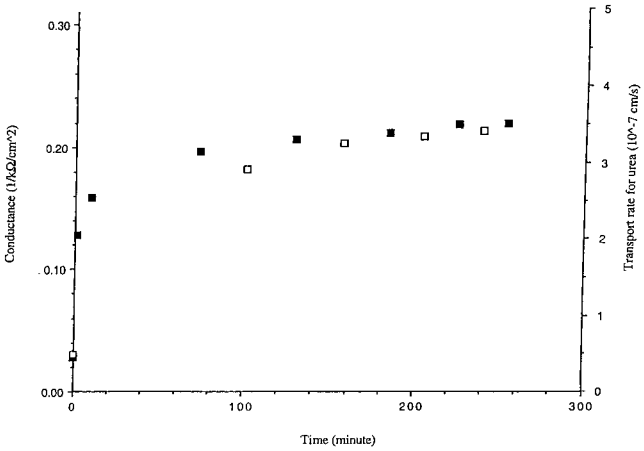

Figure 5—Representative HEM conductivity data ((kΩ cm^2)$^{-1}$), closed symbols, and HEM transport data for urea, open symbols, in study A (stage II: 3.0 V 12.5 Hz square-wave ac iontophoresis). Data are from skin sample 9.

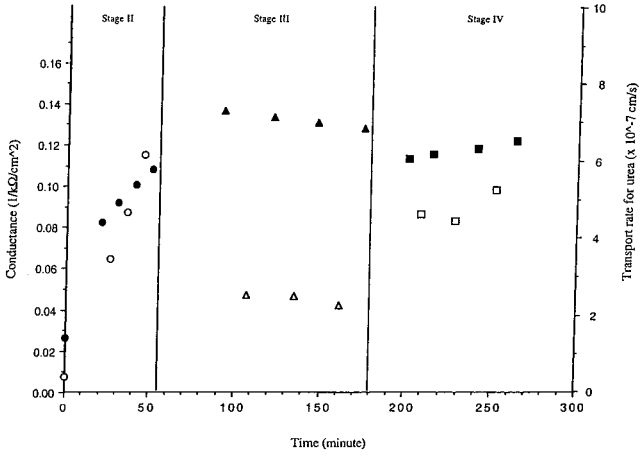

Figure 6—Representative HEM conductivity data ((kΩ cm^2)$^{-1}$), closed symbols, and HEM transport data for urea, open symbols, in study C (stage II: 2.0 V dc iontophoresis; stage III: 4.0 V 1 min followed by around 2 h 3.0 V square-wave ac iontophoresis; stage IV: superposition of 1.0 V dc and 3.0 V 12.5 Hz square-wave ac iontophoresis). Symbols: stage II, circles; stage III, triangles; stage IV, squares. Data are from skin sample 17.

Figure 6 are the relatively constant electrical resistance values and the corresponding fluxes in stages III and IV. In stage II, a lag between the increase in transport rate and the increase in conductance can be seen; this lag was noted in four of the six HEM samples of study C.

Table 1 shows the HEM electrical resistance decreases and HEM permeability increases that occurred with the modest applied 12.5 Hz square-wave ac voltages (stage II of studies A and B and stage III of study C). HEM electrical resistance and HEM permeability generally did not change by more than 25% during the conventional passive diffusion runs (stage I of studies A, B, and C). During square-wave ac iontophoresis of 2.0 to 4.0 V (stage II of studies A and B and stage III of study C), both the HEM permeability and the HEM conductance increased by up to around 30-fold relative to conventional passive diffusion runs (stage I of studies A, B, and C). Figure 7 is a plot of the Table 1 data, and it clearly reveals the relationship between the increase in HEM urea permeability and the increase in HEM electrical conductance during square-wave ac iontophoresis.

The effective pore radii estimated using the urea and mannitol flux data and the hindered transport theory in studies A and B are summarized in Table 2, and those for study C are in Table 3. The effective pore radii for HEM deduced in the passive transport experiments are consis-

Table 1—HEM Electrical Resistance (*R*) and Urea Permeability Coefficient (*P*) during 12.5 Hz Square-Wave ac Iontophoresis (stage II of studies A and B, stage III of study C) and during Passive Permeation Runs (stage I of studies A, B, and C) in Studies A, B, and C

skin sample	study	*R*, stage I (kΩ cm^2)	*P*, stage I $\times 10^8$ (cm/s)	*R*, during ac iontophoresis (kΩ cm^2)[a]	*R* ratio (*R*, stage I: *R*, during iontophoresis)	*P* ratio (*P*, during ac iontophoresis: *P*, stage I)
1	A	43	3.4	14	3.2	3.1
2	A	15	12	5.8	2.5	2.5
3	A	53	3.6	20	2.7	2.4
4	A	128	0.73	26	5	6
5	A	200	0.62	19	13	12
6	A	14	10.3	3.3	4.3	4.3
7	A	66	2.1	4.0	16	17
8	A	31	4.8	3.7	8	9
9	A	38	4.8	4.6	8	7
10	B	23	4.9	6.7	3.5	4.4
11	B	15	10.2	2.3	7	6
12	B	22	8.5	5.3	3.6	3.1
13	B	23	6.4	5.4	4.2	4.4
14	B	21	8.5	2.8	7	6
15	B	24	5.7	0.9	28	29
16	C	59	2.4	7.8	8	9
17	C	39	4.0	7.6	5	6
18	C	22	7.7	3.5	6	6
19	C	26	7.4	0.9	28	27
20	C	30	5.1	4.7	7	9
21	C	81	1.8	3.6	24	25

[a] Data taken from near the plateau region after the initial decrease (see Figures 5 and 6).

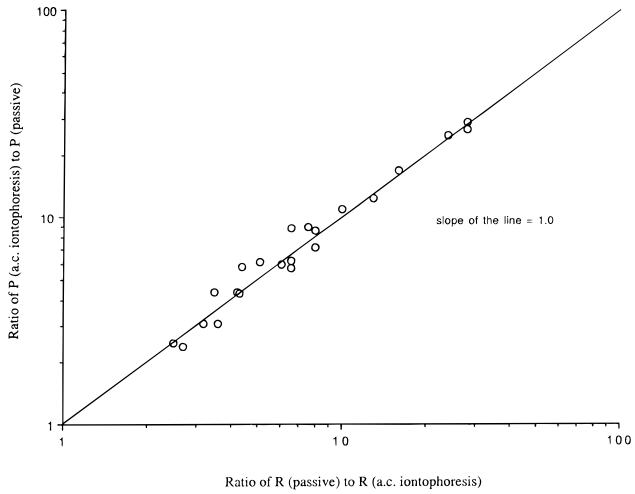

Figure 7—A correlation between the increase in HEM permeability for urea and the increase in HEM conductance in studies A, B, and C. The ratios of passive permeability to permeability during the 12.5 Hz square-wave ac iontophoresis ("passive" permeation) are plotted against the ratios of electrical conductance in passive diffusion study to the conductance in the square-wave ac iontophoresis study.

tent with those determined previously by Peck et al.[18] In Tables 2 and 3, the effective pore radii deduced for the induced pores under the electric field are seen to be of the same order of magnitude as those of the preexisting pores involved in passive diffusion. Results obtained in study B in which the extent of pore induction was expected to be increased by a 1 min dc prepulse before the square-wave ac transport run are similar to those from study A. Also seen in Table 3 are the generally somewhat smaller effective pore sizes calculated from the electroosmotic transport data obtained with continuous dc iontophoresis (stage II of study C; mean ± SD = 8.5 ± 1.4 Å, $n = 6$) when compared to those of the preexisting pores deduced from passive transport runs (stage I of studies A, B, and C; mean

Table 2—Effective Pore Radii Determined for the 12.5 Hz Square-Wave AC Iontophoresis (stage II) and Passive Permeation (stages I and III) Runs in Studies A and B

skin sample	study	protocol[a]	effective pore radius (Å)[b]		
		stage II	stage I	stage II	stage III
6	A	3 V ac	13	10	15
7	A	3 V ac	23	8.5	18
8	A	3 V ac	13	9	11
9	A	3 V ac	15	11	12
10	B	4 V dc 1 min then 3 V ac	19	9.5	12
11	B	4 V dc 1 min then 3 V ac	24	13	17
12	B	4 V dc 1 min then 3 V ac	13	13	13
13	B	4 V dc 1 min then 4 V ac	12	10	11
14	B	4 V dc 1 min then 4 V ac	13	12	13
15	B	4 V dc 1 min then 4 V ac	18	9	12.5

[a] Stages I and III were passive diffusion experiments. [b] Equation 3 was used.

$\pm$ SD $= 14 \pm 4$ Å, $n = 16$) and those deduced from the square-wave ac iontophoresis runs (stage II of studies A and B, stage III of study C; mean $\pm$ SD $= 12 \pm 2$ Å, $n = 16$). The effective radii of the pores induced by an ac electric field during square-wave ac iontophoresis (stage II of studies A and B and stage III of study C) seem to be smaller, but only marginally, than those of the preexisting pores determined in the passive diffusion runs (stage I of studies A, B, and C). The results (mean $\pm$ SD $= 8 \pm 1$ Å, $n = 6$) from stage IV of study C involving the superposition of square-wave ac (3.0 or 4.0 V) for pore induction with 1 V continuous dc as the driving force for transport (i.e., electroosmosis) were essentially the same as those from continuous dc iontophoresis alone (stage II of study C). No significant differences were observed between the effective pore radii obtained in the passive permeation runs before (stage I of studies A to C; mean $\pm$ SD $= 14 \pm 4$ Å, $n = 16$) and after the application of the electric fields (stage III of studies A and B and stage V of study C; mean $\pm$ SD $= 13 \pm 2$ Å, $n = 16$). It should be noted that the effective pore radii deduced with continuous dc iontophoresis (stage II of study C) are consistent with the results obtained in a previous study.[13] Finally, the recovery of HEM barrier properties after the application of the electric field in the ac protocol was observed to be generally faster and more complete than those after continuous dc iontophoresis (see Table 4).

Discussion

HEM Transport Studies—The effective pore sizes of HEM have important implications on the delivery of large molecules (such as oligonucleotides and polypeptides), and this has been discussed previously.[13,18] Recent findings in the effective pore sizes during low to moderate voltage iontophoresis with continuous dc electroosmotic transport may be complicated by possible variable pore surface charge density in HEM.[13] Because HEM transport enhancement with ac iontophoresis in the present experiments is basically due to the induction of new pores and not due to electroosmosis (see *Nuclepore Membrane Studies* in the *Results* section and the last paragraph in this section), possible pore charge density distributions in HEM would not affect the deduced effective pore radii with the ac protocol. Also, the same equation (eq 3) has been used in the pore radii determination with the ac iontophoresis data as in the case of the passive transport data; hence, any uncertainties arising from the use of eq 3 would likely be essentially the same for the passive and the ac situations, especially when the pore sizes are essentially the same. Thus, it is rather safe to conclude that the effective pore sizes of the pores induced in the ac experiments are close to those deduced for the preexisting pores. The situation is more complicated when the effective pore sizes deduced from the electroosmotic transport data obtained during continuous dc iontophoresis (stage II of study C) are compared to either those deduced from ac iontophoresis (stage II of studies A and B and stage III of study C) or those deduced from passive diffusion (stage I of studies A, B, and C). The smaller effective pore sizes deduced from the electroosmosis data presented in Table 3 (stages II and IV of study C) are likely the result of one or both of two possible explanations: (a) because of the directionality of the convective solvent flow during HEM electroosmosis, clearly negatively charged pores must dominate. However, there can exist a distribution of negative, positive, and neutral pores,[22] and, conceivably, negatively charged induced pores may possess smaller effective pore sizes than the neutral and/or positively charged pores; (b) the alternative explanation is that eq 4 likely has different limitations (than eq 3) in the calculation of effective pore sizes. These limitations in the region of $\lambda \geq 0.4$ have not been well investigated from the experimental standpoint[19] and raise the question of the magnitude of the actual uncertainty in the effective pore sizes presented in Tables 3 and 4 where λ values range from around 0.1 to 0.6. Only further independent studies on the quantitative applicability of eqs 3 and 4 can provide a more quantitative assessment of this issue. In the meantime, eqs 3 and 4 may be employed as a first approximation in the range of $\lambda \geq 0.4$. It is of interest to note that calculations carried out based on a mathematically more rigorous approximation of the centerline theory for $0 \leq \lambda \leq 1.0$[19] show differences of only 10 to 20% from those of eqs 3 and 4 at $\lambda \approx 0.6$.

It is noteworthy that the pore size estimates from stage II of study C are essentially the same as those from stage IV. This together with the resistance data (initial, stage II, stage III, and stage IV in Tables 1 and 3) suggest that pores induced by dc alone (stage II of study C) have characteristics similar to those induced by 12.5 Hz ac (stage IV of study C, where the 3.0 or 4.0 V ac component prevails over the 1.0 V dc component with regard to pore induction).

The correlation in Figure 7 is consistent with the results obtained in a previous study[1] and demonstrates the appropriateness of using the changes in HEM electrical resistance to represent the increase in accessible porosity/tortuosity during iontophoresis. The results in Figure 7 accordingly provide the first direct quantitative evidence of pore induction under the modest voltage conditions. Also, because the average effective pore sizes of the transport pathways during ac iontophoresis and the effective sizes of the preexisting pores are essentially the same (Tables 3 and 4), the increase in HEM permeability and the corresponding increase in HEM conductance (up to around a 30-fold increase) shown in Table 1 and Figure 7 under the ac conditions can best be interpreted as electric field induction of new pores in HEM rather than the enlargement of the preexisting pores.

Another important result of the present study is revealed in Figure 8. Here, the permeability coefficient (P) for the 12.5 Hz ac iontophoresis runs (square symbols) are plotted against electrical resistance (R) together with the corresponding conventional passive permeation data obtained before (circle symbols) and after (triangle symbols) ac iontophoresis. What is significant is that the passive permeation data fall upon the same line (slope $= -1.0$). This, together with the results in Figure 7, is further support that HEM transport enhancement under the present ac conditions is entirely due to enhanced "passive" permeation resulting from pore induction with negligible contribution from electroosmosis. The slope of -1.0 is what

Table 3—HEM Electrical Resistance (*R*) and Effective Pore Radii Determined for DC Iontophoresis (stage II), 12.5 Hz Square-Wave AC Iontophoresis (stage III), Superposition of 12.5 Hz Square-Wave AC and DC Iontophoresis (stage IV), and Passive Permeation (stages I and V) Runs in Study C

skin sample	protocol[a]			effective pore radius (Å)					*R* (kΩ cm²)[d]		
	stage II	stage III	stage IV	stage I[b]	stage II[c]	stage III[b]	stage IV[c]	stage V[b]	stage II	stage III	stage IV
16	2 V dc	4 V dc 1 min, then 3 V ac	superposition of 3 V ac with 1 V dc	10	8	12	7	12	10	7.8	8.2
17	2 V dc	4 V dc 1 min, then 3 V ac	superposition of 3 V ac with 1 V dc	11	9	13	8	14	9.6	7.6	8.3
18	2 V dc	4 V dc 1 min, then 3 V ac	superposition of 3 V ac with 1 V dc	12	10	13	8.5	15	4.1	3.5	4.7
19	3 V dc	4 V dc 1 min, then 4 V ac	superposition of 4 V ac with 1 V dc	13	7	11.5	7	11	1.0	0.9	0.71
20	3 V dc	4 V dc 1 min, then 4 V ac	superposition of 4 V ac with 1 V dc	11	10	18	9	15	6.7	4.7	6.0
21	3 V dc	4 V dc 1 min, then 4 V ac	superposition of 4 V ac with 1 V dc	10	7	11	7	9	5.0	3.6	3.2

[a] Stages I and V were passive diffusion experiments. [b] Equation 3 was used. [c] Equation 4 was used. [d] Average resistance values.

Table 4—Comparison of the Effects of Square-Wave AC and Continuous DC Iontophoresis upon the Barrier Properties of HEM in Iontophoresis Transport Studies

12.5 Hz square-wave ac protocol[a]				continuous dc[b]			
initial resistance of HEM sample (kΩ cm²)	voltage	drop in resistance[c]	recovery[d]	initial resistance of HEM sample (kΩ cm²)	voltage	drop in resistance[c]	recovery[d]
43	2 V	69	93	16	2 V	89	70
15	2 V	60	69	27	2 V	98	31
53	2 V	63	79	18	2 V	73	78
23	4 V/3 V[e]	71	92	73	2 V	92	53
15	4 V/3 V[e]	85	70	57	4 V/2 V[e]	98	40
				18	4 V/2 V[e]	95	38
24	4 V/4 V[e]	96	61	123	4 V/2 V[e]	98	12
23	4 V/4 V[e]	76	81				

[a] Duration of iontophoresis was around 2–5 h. [b] Data obtained from Li et al.;[13] duration of iontophoresis was 50 min. [c] As percent of initial electrical resistance (data from the close to plateau region after the initial decrease). [d] As percent of initial electrical resistance after the iontophoresis run when resistance became constant with time (after more than 10 h). [e] First value is the dc voltage of the 1 min prepulse and the second value is the ac voltage (in 12.5 Hz ac iontophoresis) in the present study or dc voltage (in continuous dc iontophoresis) from a previous study.[13]

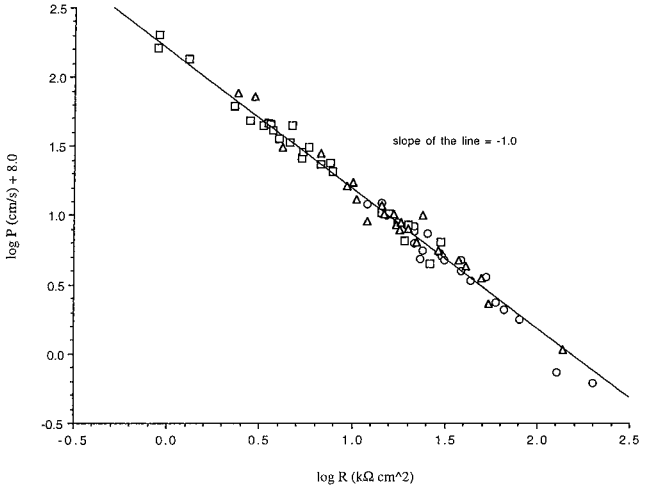

Figure 8—A correlation between HEM electrical resistance and its permeability for urea in studies A, B, and C. Symbols: passive permeation before iontophoresis, circles; 12.5 Hz square-wave ac iontophoresis ("passive" permeation), squares; passive permeation after iontophoresis, triangles.

would be expected when the transport pathways for the conducting ions in PBS during iontophoresis correlate with both the preexisting and the induced pathways for urea passive transport in HEM (see eq 9 and ref 13). The results in Figure 8 are evidence that the electrical current increases that take place during moderate voltage low-frequency ac iontophoresis is the direct result of pore induction in the stratum corneum and not due to some other transient electrical effects[5–8] such as a complex potential-dependent energy barrier for transport at the membrane–solution interface or effects arising from time dependent membrane polarization, the latter being likely important only for much shorter time frames (e.g., in the order of a millisecond[7]) than that of the present situation. These findings support the pore induction hypothesis made in previous studies with applied voltages ≥ 1 V.[1–5]

Electroporation of HEM at Low to Moderate Voltages (2 to 4 V), Yes or No—Although the issue of the sites of pore induction in human skin at low to moderate voltages is beyond the scope of the present investigation, possible mechanisms and skin morphology proposed in the literature[1,4,23–24] for the increase in skin electrical conductance observed in the present study may be discussed. Previously, Inada et al.[1] hypothesized that the increase in HEM electrical conductance at 1 to 4 V is similar to the reversible electrical breakdown found with lipid bilayer membranes and that pore formation may occur transepidermally or via the cells lining the appendageal ducts. For transepidermal electrical breakdown, the electric field across HEM under an applied potential of 2 V for an average of 15 to 20 corneocyte layers in the stratum corneum was estimated to be in the order of 40 kV/cm when the voltage drop was assumed to be concentrated across the intercellular lipid bilayers rather than the conductive corneocytes. Thinner portions of the stratum corneum may experience a higher field strength and thus may disproportionally contribute to electroporation. This calculated electric field strength (40 kV/cm) is in the order of the magnitude of, but probably at the lower end of the range of, field strengths needed to induce electrical breakdown of lipid bilayer membranes, estimated to be around 50 to 200 kV/cm based on a bilayer thickness of around 10 nm and a "threshold voltage" of around 50 to 200 mV over periods of seconds[25,26] to minutes.[27] The "threshold" voltage used in the above estimation for membrane electroporation is strongly dependent on the duration of the applied electric field and the particular type of the membrane. The view of reversible breakdown of the epithelial cell bilayers lining the appendages was offered earlier by Kasting and Bow-

man[5] as a possible explanation for the time-dependent, nonlinear, current−voltage relationship observed in their skin electrical resistance study. The number of bilayers involved in this case is much smaller than that of full thickness stratum corneum, and accordingly the electric field strengths attainable in the bilayers lining the appendages could be much greater and much more than sufficient to induce electroporation. Chizmadzhev et al.[23] has come to a similar conclusion in a recent quantitative examination of this problem. Under applied potentials of a few volts, Chizmadzhev et al. state that the "time-dependent, nonlinear current−voltage characteristics of the skin can be attributed to electroporation" associated with the epithelial cells lining skin appendages. Their analysis "confirms skin electroporation at low voltages", which is in agreement with the views of Kasting and Bowman[5,6] and Inada et al.[1] The results in Figures 7 and 8 of the present study clearly support electroporation at these low to moderate voltage conditions.

Pulsed and Continuous Iontophoresis—Although pulsed dc iontophoresis transport experiments were not conducted in the present investigation, the results of the present HEM electrical resistance study impact upon the understanding of pulsed dc iontophoresis, and some discussion here is instructive. Pulsed dc iontophoresis has been an aspect of interest in transdermal iontophoresis partly because of the possible advantage of less skin irritation than that with continuous dc iontophoresis[28,29] and the belief by some researchers that it may provide greater transport enhancement than conventional continuous dc iontophoresis via mechanisms that are unique in pulsed iontophoresis.[30] Some previous studies have reported that higher or equal fluxes are observed under continuous dc iontophoresis relative to pulsed dc iontophoresis,[7,29,31−32] but other studies have suggested higher transport rates or greater pharmacological effects under pulsed dc iontophoresis.[33,34] These differing results demonstrate the need for more systematic mechanistic studies to compare the effects of pulsed dc and continuous dc upon the barrier properties of skin.

Results from the present electrical resistance study can provide a better understanding of the mechanism(s) of pore induction in human skin during pulsed and/or continuous dc iontophoretic enhanced transdermal delivery. A particular advantage of the protocols used in the present study has been that of minimizing the influence of skin-to-skin variabilities. By utilizing the same HEM sample for successive experiments, the influence of the variabilities has been reduced and more meaningful results were obtainable. The merit of this approach is illustrated by the relatively small data scatter in Figure 3 (contrast this with the large variations seen in Table 4 for the effects of pulsed dc and continuous dc on the barrier properties of HEM).

Because HEM conductance was shown to be directly proportional to the "passive" permeability of HEM (Figures 7 and 8), the electrical conductance results presented in Figure 3 suggest that continuous dc iontophoresis generally induces a greater extent of pore induction than those observed during pulsed dc and ac iontophoresis at the same level of applied voltage (2.0 to 3.0 V) and duration. The present electrical conductance data are consistent with the study by Yamamoto and Yamamoto.[35] The generally larger extent of pore induction in HEM observed during continuous dc iontophoresis than in pulsed and ac iontophoresis under the applied voltage conditions in the present study is believed to be at least in part due to the depolarization/recovery of the membrane allowed between each ac square-wave pulse and is consistent with the hypothesis of pore induction at the bilayer level in HEM. The dc square-wave pulsed iontophoresis (with a 1, 2, or 3 ms delay between each pulse) induced a lesser extent of pore induction than those by continuous dc (Figure 3) and approached those by 12.5 Hz square-wave ac; this also supports the hypothesis that depolarization between the pulses (ac or dc) allows for depolarization/recovery of the membrane during iontophoresis, and hence, lessen the extent of pore induction. This depolarization/recovery between pulses may also lead to the observed faster (data not shown) and more complete (Table 4) recovery of HEM barrier properties after ac and pulsed dc iontophoresis than those after continuous dc iontophoresis. It should be noted that the results presented in Figure 3 are for the particular case of consecutive 10 s runs, and the differences between continuous dc and pulsed dc are rather modest. For longer duration and at higher applied voltages, there may be greater differences between continuous dc and pulsed dc and/or ac. More work is needed in this area.

References and Notes

1. Inada, H.; Ghanem, A.-H.; Higuchi, W. I. Studies on the effects of applied voltage and duration on human epidermal membrane alteration/recovery and the resultant effects upon iontophoresis. *Pharm. Res.* **1994**, *11*, 687−697.
2. Sims, S. M.; Higuchi, W. I.; Srinivasan, V. Skin alteration and convective solvent flow effects during iontophoresis: I. neutral solute transport across human skin. *Int. J. Pharm.* **1991**, *69*, 109−121.
3. Sims, S. M.; Higuchi, W. I.; Srinivasan, V. Skin alteration and convective solvent flow effects during iontophoresis: II. monovalent anion and cation transport across human skin. *Pharm. Res.* **1992**, *9*, 1402−1409.
4. Keister, J. C.; Kasting, G. B. A kinetic model for ion transport across skin. *J. Membr Sci.* **1992**, *71*, 257−271.
5. Kasting, G. B.; Bowman, L. A. Electrical analysis of fresh, excised human skin: a comparison with frozen skin. *Pharm. Res.* **1990**, *7*, 1141−1146.
6. Kasting, G. B.; Bowman, L. A. DC electrical properties of frozen, excised human skin. *Pharm. Res.* **1990**, *7*, 134−143.
7. Bagniefski, T.; Burnette, R. R. A comparison of pulsed and continuous current iontophoresis. *J. Controlled Release* **1990**, *11*, 113−122.
8. Dinh, S. M.; Lao, C. W.; Berner, B. Upper and lower limits of human skin electrical resistance in iontophoresis. *AIChE J.* **1993**, *39*, 2011−2018.
9. Prausnitz, M. R. The effects of electric current applied to skin: a review for transdermal drug delivery. *Adv. Drug Deliv. Rev.* **1996**, *18*, 395−425.
10. Jadoul, A.; Preat, V. Electrically enhanced transdermal delivery of domperidone. *Int. J. Pharm.* **1997**, *154*, 229−234.
11. Pliquett, U.; Langer, R.; Weaver, J. C. Changes in passive electrical properties of human stratum corneum due to electroporation. *Biochim. Biophys. Acta* **1995**, *1239*, 111−121.
12. Vanbever, R.; Boulenge, E. L.; Preat, V. Transdermal delivery of fentanyl by electroporation I. Influence of electrical factors. *Pharm. Res.* **1996**, *13*, 559−565.
13. Li, S. K.; Peck, K. D.; Ghanem, A.-H.; Higuchi, W. I. Characterization of the transport pathways induced during low to moderate voltage iontophoresis in human epidermal membrane. *J. Pharm. Sci.* **1998**, *87*, 40−48.
14. Peck, K. D.; Ghanem, A.-H.; Higuchi, W. I. The effect of temperature upon the permeation of polar and ionic solutes through human epidermal membrane. *J. Pharm Sci.* **1995**, *84*, 975−982.
15. Srinivasan, V.; Higuchi, W. I.; Su, M.-H. Baseline studies with the four-electrode system: the effect of skin permeability increase and water transport on the flux of a model uncharged solute during iontophoresis. *J. Controlled Release* **1989**, *10*, 157−165.
16. Peck, K. D.; Ghanem, A.-H.; Higuchi, W. I.; Srinivasan, V. *Int. J. Pharm*. Improved stability of the human epidermal membrane during successive permeability experiments. **1993**, *98*, 141−147.
17. Tregear, R. T. *Physical Functions of Skin*. Academic Press: New York, 1966; pp 53−57.
18. Peck, K. D.; Ghanem, A.-H.; Higuchi, W. I. Hindered diffusion of polar molecules through and effective pore radii estimates of intact and ethanol treated human epidermal membrane. *Pharm. Res.* **1994**, *11*, 1306−1314.
19. Deen, W. M. Hindered transport of large molecules in liquid-filled pores. *AlChE. J.* **1987**, *33*, 1409−1425.

20. Sandifer, J. R. *Ion-Transfer Kinetics: Principles and Applications*, VCH: New York, 1995; Ch. 4.
21. Peck, K. D.; Srinivasan, V.; Li, S. K.; Higuchi, W. I.; Ghanem, A.-H. A quantitative description of the effect of molecular size upon electroosmotic flux enhancement during iontophoresis for a synthetic membrane and human epidermal membrane. *J. Pharm. Sci.* **1996**, *85*, 781−788.
22. Pikal, M. J. *Pharm. Res.* Transport mechanisms in iontophoresis. I. A theoretical model for the effect of electroosmotic flow on flux enhancement in transdermal iontophoresis. **1990**, *7*, 118−126.
23. Chizmadzhev, Y. A.; Indenbom, A. V.; Kuzmin, P. I.; Galichenko, S. V.; Weaver, J. C.; Potts, R. O. Electrical properties of skin at moderate voltages: contribution of appendageal macropores. *Biophys. J.* **1998**, *74*, 843−856.
24. Chizmadzhev, Y. A.; Zarnitsin, V. G.; Weaver, J. C.; Potts, R. O. Mechanism of electroinduced ionic species through a multilamellar lipid system. *Biophys. J.* **1995**, *68*, 749−765.
25. Chang, D. C.; Chassy, B. M.; Saunders: J. A.; Sowers, A. E. *Guide to Electroporation and Electrofusion*; Academic Press: New York, 1992.
26. Neumann, E.; Sowers, A. E.; Jordan, C. A. *Electroporation and Electrofusion in Cell Biology*; Plenum Press: New York, 1989.
27. Donlon, J. A.; Rothstein, A. The cation permeability of erythrocytes in low ionic strength media of various tonicities. *J. Membr. Biol.* **1969**, *1*, 37−52.
28. Okabe, K.; Yamaguchi, H.; Kawai, Y. New iontophoretic transdermal administration of the beta-blocker metoprolol. *J. Controlled Release* **1986**, *4*, 79−85.
29. Hirvonen, J.; Hueker, F.; Guy, R. H. Current profile regulates iontophoretic delivery of amino acids across the skin. *J. Controlled Release* **1995**, *37*, 239−249.
30. Pikal, M. J.; Shah, S. Study of the mechanisms of flux enhancement through hairless mouse skin by pulsed dc iontophoresis. *Pharm. Res.* **1991**, *8*, 365−369.
31. Numajiri, S.; Sakurai, H.; Sugibayashi, K.; Morimoto, Y.; Omiya, H.; Takenaka, H.; Akiyama, N. Comparison of depolarizing and direct current systems on iontophoretic enhancement of transport of sodium benzoate through human and hairless rat skin. *J. Pharm. Pharm.* **1993**, *45*, 610−613.
32. Preat, V.; Thysman, S. Transdermal iontophoretic delivery of sufentanil. *Int. J. Pharm.* **1993**, *96*, 189−196.
33. Knoblauch, P.; Moll, F. In vitro pulsatile and continuous transdermal delivery of buserelin by iontophoresis. *J. Controlled Release* **1993**, *26*, 203−212.
34. Liu, J. C.; Sun, Y.; Siddiqui, O.; Chien, Y. W.; Shi, W.-M.; Li, J. Blood glucose control in diabetic rats by transdermal iontophoresis delivery of insulin. *Int. J. Pharm.* **1988**, *44*, 197−204.
35. Yamamoto, T.; Yamamoto, Y. Nonlinear electrical properties of skin in the low-frequency range. *Med. Biol. Eng. Comput.* **1981**, *19*, 302−310.

Acknowledgments

This research is supported by NIH Grant GM 43181 and an Advanced Predoctoral Fellowship in Pharmaceutics awarded to S. Kevin Li from the Pharmaceutical Research and Manufacturers of America Foundation. The authors thank Professor Paul C. Fife for helpful discussion and TheraTech, Inc. for supplying the human epidermal membrane.

JS980331Y